Pis'ma v ZhETF, vol. 79, iss. 4, pp. 218 – 222 © 2004 February 25

Anti-crossing phenomena in a resonator with 2D electrons on liquid helium

J. Klier, A. Würl, V. Shikin[+]

Fakultät für Physik, Universität Konstanz, 78457 Konstanz, Germany

[+]*Institute of Solid State Physics RAS, 142432 Chernogolovka, Moscow District, Russia*

Submitted 22 January 2004 г.

We have investigated the details of the eigenmode for a resonator containing a two-dimensional electron system (2DES), formed on the surface of liquid helium. We show that anti-crossing phenomena occur near the crossing point $\omega_0 = \omega_c$, where ω_0 is the eigenmode of the resonator and ω_c is the cyclotron frequency. The structure of the coupling constant is established. It is a flexible parameter, i.e., sensitive especially to magnetic field and electron density. A finite coupling leads to a perturbation, $\delta\omega$, of the eigenmode of the resonator in presence of the 2DES. Corresponding calculations and measurements of $\delta\omega$ are presented. The theory fits the experimental data. The influence of anti-crossing on the cyclotron resonance absorption line-shape is demonstrated.

PACS: 67.70.+n, 72.10.−d, 72.60.+g, 73.50.−h

Cyclotron resonance (CR) measurements in magnetic fields represent a valuable method to study the electronic properties of two-dimensional electron systems (2DES). In low density electron systems the CR is usually investigated by using a resonator cavity, see e.g. Refs. [1, 2, 3, 4, 5, 6, 7, 8]. Under these conditions the CR of the electrons appears when the requirement

$$\omega_0 = \omega_c \tag{1}$$

is fulfilled. Here ω_0 is the resonator eigenmode and $\omega_c = (eB)/(m_e c)$ is the electron cyclotron frequency in magnetic field B, m_e is the free electron mass, e the elementary charge, and c is the velocity of light.

However, this condition is only correct in the limiting case $n_s \to 0$, where n_s is the average density of the 2DES. If $n_s \neq 0$ then the coupling between the resonator mode and the 2DES becomes important due to the development of anti-crossing mode repulsion around the crossing point $\omega_0 = \omega_c$ (1). The effect of anti-crossing in the system 'resonator + 2DES' is similar to well-known phenomena, e.g., the pre-dissociation effect in the behaviour of diatomic molecules [9], the dispersion of the dielectric constant near atomic oscillator eigenmodes [10], energy gaps in the free electron spectrum caused by periodical potential perturbation [10, 11], the so-called polariton effect in dielectrics [12], etc. It has surmised to be fixed in any CR measurements Refs. [1 – 8], however, this effect was not discussed so far (to be correct see comment [13]). Here we present a detailed analysis of this problem and show the influence of anti-crossing phenomena in CR absorption measurements.

The main information about 'anti-crossing' is extracted from measurements of the shift of the eigenmode of the resonator, $\delta\omega$, caused by the presence of a 2DES. For these investigations the setup shown in the inset in Fig.1 has been used. Details of this setup are discussed in Ref. [8].

The resonator eigenmode is determined by the position of the maximum of the transmission signal. Examples of such signal structures are presented in Fig.1. A typical set of data for ω_e, the eigenmode of the resonator in presence of electrons, as function of B and electron density n_s is shown in Fig.2. These data can be understood as a combination of two contributions, i.e.,

$$\omega_e = \omega_0 + \delta\omega \ , \quad \text{with} \quad \delta\omega = \delta\omega_\sigma + \delta\omega_p \ , \tag{2}$$

where ω_0 is the eigenmode of the empty resonator with just the Si substrate inside it (at fixed liquid helium level and electric field $E_\perp = 0$), see Fig.1.

The first contribution, $\delta\omega_\sigma$, is due to the finite conductivity of the 2DES. In the limiting case, when the coupling constant $\sigma \ll 1$ (the definition of σ is shown below in Eq. (8)), the shift $\delta\omega_\sigma$ is a linear function of n_s (at least when $B \to 0$). So we obtain

$$\delta\omega_\sigma(n_s, B)|_{B\to 0} \propto n_s \ , \quad \delta\omega_\sigma(n_s, B)|_{B\to\infty} \to 0. \tag{3}$$

The second contribution in $\delta\omega$, $\delta\omega_p$, results from the sensitivity of the eigenmode on the liquid helium level and $E_\perp$ in the resonator (the electric pressing field applied to the Si substrate). Such a shift is not sensitive to magnetic field and has a non-linear dependence on n_s.

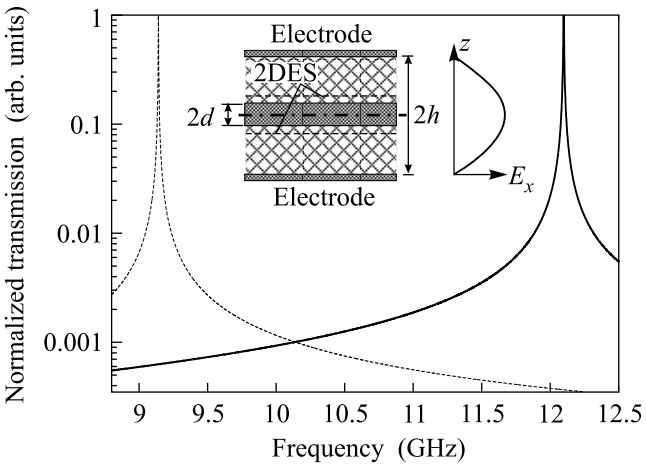

Fig.1. The measured transmission signals for the empty resonator (solid line) and for the system 'resonator + Si' (dashed line), with eigenmodes ω_{empty} and ω_0 respectively. Inset: Schematical sketch of the cavity and, at the center, of the dielectric Si substrate with a helium film around it (the total thickness is $2d$). Two high frequency coax-lines, not shown, are connected left and right to the resonator to apply the microwave excitation to the system 'resonator + 2DES' and measure its transmitted signal. $2h$ is the distance between the upper and lower electrodes. On the right a typical profile of the electric field, E, is shown

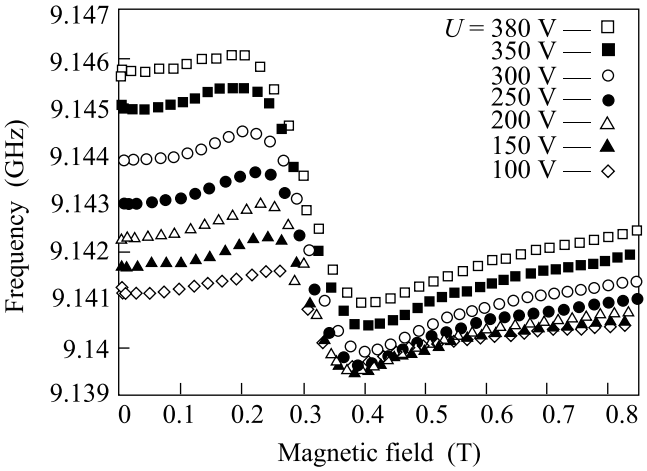

Fig.2. The measured dependence of ω_e versus B for several electron densities. The experimental conditions correspond to a saturation density of the 2D electron layers on the bulk helium surface. Therefore $n_s \propto U$, where U is the potential difference between the Si substrate and the cavity. Here $U_{\text{crit}} = 384$ V, i.e., this potential corresponds to the maximum charge density, $n_s^{\text{crit}} = 2 \times 10^{12}\text{m}^{-2}$, on a bulk helium surface due to the electro-hydrodynamical instability

Using Eqs. (2) and (3) we can renormalize the experimental data presented in Fig.2. The results are shown

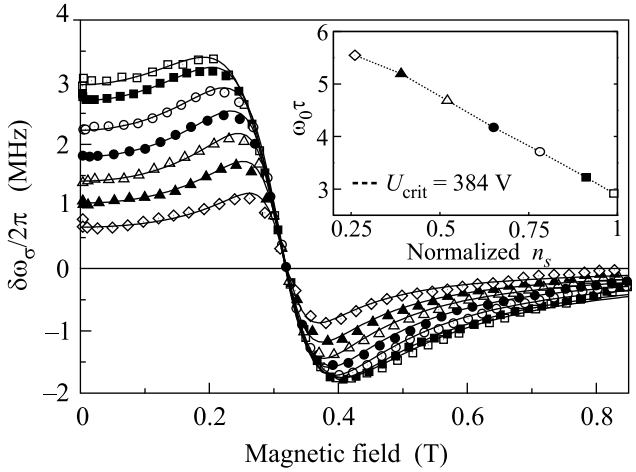

Fig.3. The dependence of $\delta\omega_\sigma$ versus B. $\delta\omega_\sigma$ is extracted from the measured data in Fig. 2 using Eqs. (2) and (3). The solid lines represent the fits to the data using Eq. (10) and the relaxation time τ as fitting parameter. Inset: The dependence of $\omega_0\tau$ on n_s after the fitting program, Eq. (10), has been realized. Here the data are normalized to the maximum density, at $U_{\text{crit}} = 384$V

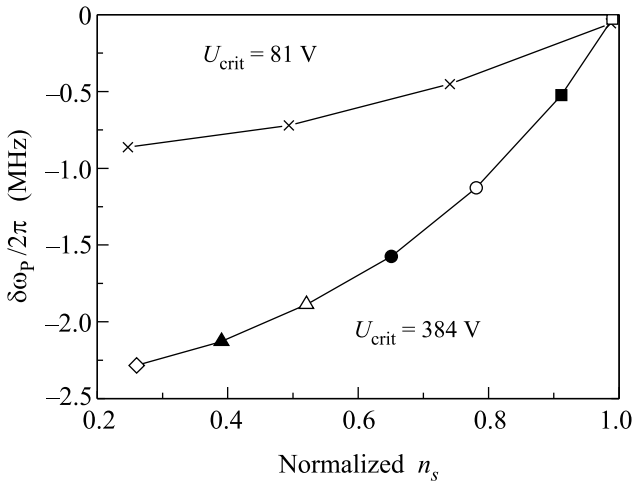

Fig.4. The shift $\delta\omega_p$ vs normalized electron density ('1' along the horisontal axis corresponds to the given critical value of n_s^{crit}). The lower line corresponds to the data shown in Figs.2 and 3, when $U_{\text{crit}} = 384$ V. The upper line shows $\delta\omega_p$ measured for a thinner bulk helium film, with $U_{\text{crit}} = 81$ V. The observed dependence reflects the sensitivity of the transmission signal to the helium level, i.e., the electron pressure P_{el} is proportional to U^2. So $\delta\omega_p$ is a non-linear function of U

in Fig.3 and 4. Fig.3 presents the shift $\delta\omega_\sigma$ versus B. It is evident that the distribution $\delta\omega_\sigma$ follows the requirements in (2) and (3): $\delta\omega_\sigma$ is additive with $\delta\omega_p$, Fig.4, is linear dependent on n_s, and goes to zero when $B \to \infty$.

To check the properties of $\delta\omega_p$ we have plotted its dependence against the normalized electron density, see Fig.4. As indicated above, the shift $\delta\omega_p$ includes two effects. One of them corresponds to a decreasing eigenmode when $E_\perp \neq 0$ (without the presence of electrons, i.e., $n_s = 0$). In this case the electric field lifts the helium level and so the eigenmode goes down (see Fig.1). The other effect, when $n_s \neq 0$, arises from the electron pressure, $P_{el} \propto eE_\perp n_s$, which pushes the helium level down and hence the eigenmode increases (see Fig.4). Variances of this shift has been discussed [14].

To explain the data in Fig.3 we need the dispersion calculated for the model setup, inset in Fig.1. The Maxwell equations for the E-mode with

$$E_z = 0, \quad E_y = 0, \quad E_x \neq 0, \tag{4}$$

are completed by the boundary conditions. The electric fields are zero for $z = \pm h$. Along the boundaries $z = \pm d$ of the Si layer we have to equate E_x from both sides of these boundaries.

It is also necessary to take into account the contribution arising from the presence of the movable 2DES. The 2D electrons are localized along the helium film, with thickness $d_{\rm He}$, above the Si substrate. Typically $d_{\rm He} < d$, where $2d$ is the thickness of the Si substrate (see inset in Fig.1) and $(\epsilon_{\rm He} - 1) \ll (\epsilon_{\rm Si} - 1)$. Therefore, and for simplification, we neglect the existence of $d_{\rm He}$. $\epsilon_{\rm He}$ and $\epsilon_{\rm Si}$ are the dielectric constant of liquid helium and the Si substrate. As result we have along the Si substrate a jump of the magnetic field, caused by 2D electron motion,

$$H_y^{vac}(d) - H_y^{Si}(d) = \frac{4\pi j_x(d)}{c}, \tag{5}$$

with

$$j_x = en_s v_x, \tag{6}$$
$$\left(i\omega + \frac{1}{\tau}\right) v_x = \frac{eE_x}{m_e} + \omega_c v_y, \quad \left(i\omega + \frac{1}{\tau}\right) v_y = -\omega_c v_x,$$

where v_x and v_y are the components of the electron velocity, and τ is the momentum relaxation time.

Based on these calculations we can formulate the dispersion law as

$$\tan(qd) - \frac{\sin(kd) + \cos(kd)\cot(kh)}{\cos(kd) - \sin(kd)\cot(kh)} = \frac{4\pi i}{c}\,\sigma_{xx}\ , \tag{7}$$

where $k^2 = \dfrac{(\omega_{\rm e} - \delta\omega_p)^2}{c^2}$ and $q^2 = \epsilon_{\rm Si}\dfrac{(\omega_{\rm e} - \delta\omega_p)^2}{c^2}$.

σ_{xx} is the *ac* conductivity of the 2DES in magnetic field. Again because the thickness of the helium film is much less than d it is not important for the definition of $\omega_{\rm e}$. The result (7) has been published in [14], but without considering magnetic field.

The conductivity $\sigma_{xx}(\omega, \omega_c)$ of the 2DES is described by the conventional *ac* Drude form

$$\sigma_{xx} = \sigma'_{xx} + i\sigma''_{xx}\ ,$$
$$\text{with} \quad \sigma'_{xx} = \sigma'(\omega\tau, \omega_c\tau)\ , \quad \sigma''_{xx} = \sigma''(\omega\tau, \omega_c\tau)\ ,$$

where ω is the external pumping frequency.

From Eq. (7) it becomes evident, that the coupling constant σ is defined as

$$\sigma = \frac{4\pi i}{c}\,\sigma_{xx}\ . \tag{8}$$

If σ is small enough ($\sigma \ll 1$) then the general expression, Eq. (7), can be simplified, i.e.,

$$\tan(q_0 d) - \frac{\sin(k_0 d) + \cos(k_0 d)\cot(k_0 h)}{\cos(k_0 d) - \sin(k_0 d)\cot(k_0 h)} = 0 \tag{9}$$
$$\text{with} \quad k_0^2 = \frac{\omega_0^2}{c^2} \quad \text{and} \quad q_0^2 = \epsilon_{\rm Si}\frac{\omega_0^2}{c^2}\ .$$

$$h\delta\omega'_\sigma = 4\pi\ \sigma''_{xx}(\omega_0, \omega_c)\ f\ , \tag{10}$$
$$h\delta\omega''_\sigma = 4\pi\ \sigma'_{xx}(\omega_0, \omega_c)\ f\ , \tag{11}$$
$$f = \cos(k_0 d)\sin(q_0 d)\frac{\tan(k_0 d)\tan[d(q_0 - k)] - 1}{\cos[d(q_0 - k)]}\ .$$

We can see that in linear approximation, when $\sigma \ll 1$, the shift $\delta\omega$ is proportional to the imaginary part of the conductivity, i.e., $\delta\omega'_\sigma \propto \sigma''_{xx}$. Such a dependence fits the experimental data for $\delta\omega_\sigma$, with the normalization in one point, see Fig.3. Normalization allows to circumvent the lack of knowledge of the electron density n_s and the geometrical factor f. Results similar to Eqs. (10) and (11), but for a different resonator geometry, have been obtained in Ref. [15].

From successful fitting the data (solid lines in Fig.3) we can conclude: (a) Eq. (2) is a reasonable presentation for $\delta\omega$, (b) the geometrical factor f in Eqs. (10) and (11) is not sensitive to both n_s and B, and (c) the scale of the coupling constant σ, Eq. (8), is far from the resonance condition small enough. Using the data in Fig.3 and an estimation of n_s via $U/d \sim en_s$, we can conclude that

$$0.01 < \text{Re}\ \sigma|_{B\to 0} < 0.04\ , \tag{12}$$

where σ is from Eq. (8). This estimation is consistent with the simplifications Eqs. (9) to (11). It also indicates that the quality of the eigenmode peaks in the reflection

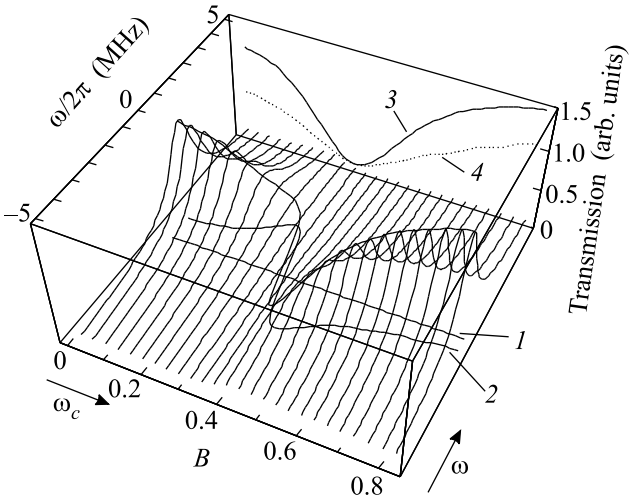

Fig.5. Frequency scans, ω-axis, as function of the applied magnetic field B (along this axis ω_c is determined). Each scan represents a measured transmission signal, $T(\omega, B)$, with the dependence of the maxima and signal shape on $\sigma''_{xx}(B)$. The trace in the ω, B plane (line 1) corresponds to the condition $\omega = \omega_0$. Line 2 exhibits the path of the frequency at the maxima of the transmission lines. Details of this line are presented in Fig.3. The trace in the B, T-plane (line 3) represents the CR absorption under optimal conditions, i.e., the maxima of the transmission signals. Line 4 reflects the situation for a fixed frequency, i.e., $\omega = \omega_c$, during the CR absorption measurements

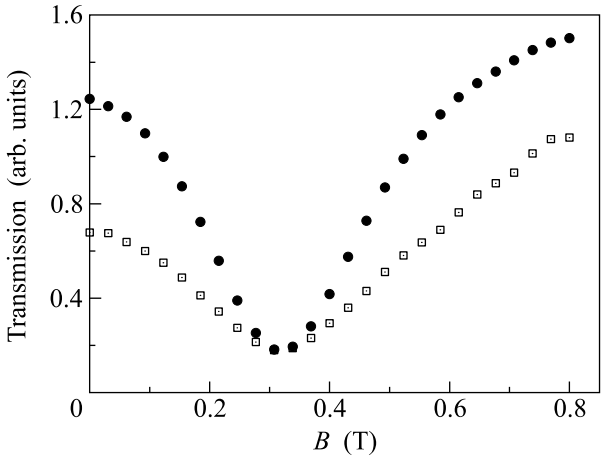

Fig.6. A comparison of transmission vs magnetic field for CR measurements with fixed ω (open symbols) and flexible ω (solid symbols)

(or transmission) data is much better than for the CR-line shape.

In Fig.5 the general experimental picture of the transmission signal T, for the setup shown in the inset in Fig.1, is presented as a function of B and ω. The profiles of $T(\omega, B)$ for fixed B but changing ω clearly show pronounced eigenmode peaks. The position of these peaks in the ω, B-plane follows line 2, formed in the vicinity of line 1 with $\omega = \omega_0$.

The quality of the peaks of the eigenmode goes down in the vicinity of the anti-crossing area. The trace of the $T(\omega, B)$ profile in the ω, T-plane corresponds to the information of the CR absorption. This trace is quite sensitive to the conditions of the projection.

Using the $T(\omega, B)$ presentation, Fig.5, we can explain in details the information Fig.6. The 'solid' and 'open' symbols correspond to projections of the $T(\omega, B)$ profile to the plane (T, B) (lines 3 and 4 in Fig.5). Certainly the optimal experimental path corresponds to line 3.

In conclusion we have demonstrated and explained the existence of anti-crossing phenomena in the system 'resonator + 2DES'. The scale of the coupling constant σ, Eq. (8), is deduced from the data (12). The coupling is flexible (it is sensitive to both magnetic field and electron density). Such a flexibility reduces $\delta\omega_\sigma$ to zero at the crossing-point $\omega_0 = \omega_c$. However, in the vicinity of this point the shift $\delta\omega_\sigma$ exists and can be measured. The experimental verification of the anti-crossing phenomena is shown in Figs.3 and 5. It looks as a $\delta\omega(B)$ shift, which is similar to the dielectric constant dispersion in optics (see Refs. [9, 10]). The general picture of the transmission signal versus ω and B in the presence of anti-crossing phenomena is discussed, see Fig.5. The details of the anti-crossing cyclotron resonance line shift $\delta\omega_\sigma$ are investigated. The measured data of $\delta\omega_\sigma$ follow the predictions, Eq. (9), quite well, see Fig.3. The coupling between anti-crossing phenomena and behaviour of the CR absorption line width is discussed. The optimal way to measure such a line shape is indicated (see 'solid' symbols in Fig.6 and line 3 in Fig.5).

We thank P. Leiderer for informative discussions. This activity is supported by the DFG, Forschergruppe 'Quantengase', the EU-RTN 'Surface electrons on mesoscopic structures', and RFBI 03-02-16121.

1. G. Dresselhaus, A.F. Kip, and C. Kittel, Phys. Rev. **98**, 368 (1955).
2. T.R. Brown and C.C. Grimes, Phys. Rev. Lett. **29**, 1233 (1972).
3. V. Edel'man, Pis'ma ZhETF **24**, 510 (1976) [JETP Lett. **24**, 468 (1976)]; Pis'ma ZhETF **26**, 647, (1977) [JETP Lett. **26**, 493 (1977)].
4. V. Edel'man, ZhETF **77**, 673, (1979) [Sov. Phys. JETP **50**, 338 (1979)].
5. L. Wilen and R. Giannetta, Phys. Rev. Lett. **60**, 231 (1988).

6. E. Teske, Yu. Monarkha, M. Seck, and P. Wyder, Phys. Rev. Lett. **82**, 2772 (1999).
7. Yu. Monarkha, E. Teske, and P. Wyder, Phys. Rev. B **59**, 14884 (1999); *ibid* **62**, 2593 (2000).
8. J. Klier, A. Würl, P. Leiderer et al., Phys. Rev. **B65**, 165428 (2002); and references therein.
9. L. Landau and E. Lifshitz, *Quantum mechanics*, Pergamon Press, 1977, p. 347.
10. see, e.g., J. Ziman, *Principle of the theory of solids*, Cambridge University Press, 1964, p. 269.
11. N. Ashcroft and N. Mermin, *Solid State Phyiscs*, Saunders College Publishing, 1976, p. 826.
12. H. Raether, *Excitations of plasmons and interband transitions by electrons*, Springer Berlin, 1980.
13. In Ref. [5], the existence of the anti-crossing problem for the system 'resonator + 2DES' has been indicated (see comments in their Ref. [7]). However, there is no information with respect to $\delta\omega$ caused by anti-crossing phenomena (neither theoretically nor experimentally).
14. A. Würl, J. Klier, P. Leiderer, and V. Shikin, J. Low Temp. Phys. **126**, 511 (2002).
15. V. Shikin, Pis'ma ZhETF **75**, 31 [JETP Lett. **75**, 29 (2002)].